International Journal of Rock Mechanics & Mining Sciences 47 (2010) 1046–1054

Contents lists available at ScienceDirect

International Journal of Rock Mechanics & Mining Sciences

journal homepage: www.elsevier.com/locate/ijrmms

Technical Note

Case study of blast-induced shock wave propagation in coal and rock

Cai-Ping Lu [a,b,*], Lin-Ming Dou [a,b], Xing-Rong Wu [c], Yao-She Xie [a,b]

[a] State Key Laboratory of Coal Resources and Mine Safety, China University of Mining and Technology, Xuzhou, Jiangsu 221008, PR China
[b] School of Mining Engineering, China University of Mining and Technology, Xuzhou, Jiangsu 221008, PR China
[c] Sanhejian Mine of Xuzhou Coal Mining Group, Xuzhou, Jiangsu 221613, PR China

ARTICLE INFO

Article history:
Received 26 August 2009
Received in revised form
8 March 2010
Accepted 13 June 2010
Available online 1 July 2010

1. Introduction

The propagation and attenuation laws of blast-induced shock wave in coal and rock are always one of the key research topics in geophysics and geotechnical engineering. When a blast-induced shock wave propagates in a single medium, it will be attenuated by geometric spreading. Simultaneously, because of the plasticity, non-linear and viscous damping actions of the coal and rock materials, etc., the energy of shock wave will be rapidly attenuated. But when a shock wave propagates in a layered seam, undergoing the coal and rock surface refraction and reflection process, the energy loss level is consistent with the surface characteristics, the coal and rock wave impedance of both sides of surface, the propagation direction, and the surface angle. In summary, blast-induced shock wave propagation in coal and rock materials is a very complicated question, which still cannot be interpreted by a unified expression in theory.

Previous research focusses mainly on blast-induced shock wave propagation and attenuation laws in different media, as well as the stability and safety evaluation of buildings on surface. For example, AK et al. [1] discovered that 98% of the frequency values of blasting signals were between 4 and 40 Hz, and established the relationship between the peak particle velocity (PPV) and the frequency spectrum, when he studied ground vibration measurement induced by bench blasting at Magnesite Incorporated Company (MAS) open pit mine in Turkey. Tantawy [2] proposed an artificial neural network (ANN) for prediction and control of the blast-induced shocks in Assiut (Egypt) limestone quarry, and established three different models of ANN used in predicting the PPV. Holub and Petroš [3] discovered that the PPV nearby the stations and the main frequency can reveal the mechanic parameters of the coal and rock materials, and they are the best criteria to assess the vibration damage to the surface structures and in mines, by a total of 240 three-component recordings from 80 rockbursts, which occurred in various coal mines in the Ostrava-Karviná Coal Basin. Wu et al. [4] realized that the main frequency of the blast-induced shock wave can be used to assess the stability and safety of the structures, when studied the propagation characteristics of blast-induced shock waves in a jointed rock mass, simultaneously revealed the main frequency attenuation law of the shock waves in relation to propagation distance, the charge weight and the incident angle. Kuzu [5] studied the blast-induced shock wave attenuation law in relation to the charge weight and the propagation distance based on 60 shots in a sandstone quarry area near Kemerburgaz in Istanbul, and proposed the prediction model of PPV, namely when the main frequency values were below 40 Hz to bring the PPV to a safe level (18.75 mm/s). Khandelwal and Singh [6] proposed a new neural network for the prediction of ground vibration and frequency by all possible influencing parameters of rock mass, explosive characteristics and blast design, and discovered that the corresponding coefficients of correlation are 0.9994 and 0.9868, respectively. Wang et al. [7] analyzed the attenuation of sound-wave propagation in the rock samples before and after impact tests based on light gas gun (LGG) tests. Hao et al. [8] investigated the rock joint effects on stress wave propagation, and discussed the effects of rock joints on characteristics of stress wave propagation such as peak value attenuation, spectrum, and spatial variations. Uysal et al. [9] measured PPV values by two instruments located just in front of and behind the empty barrier holes, and investigated the effect of empty barrier holes alone on seismic vibration. Khandelwal and Singh [10] evaluated and

* Corresponding author at: School of Mining Engineering, China University of Mining and Technology, Xuzhou, Jiangsu 221008, PR China.
Tel.:/fax: +86 51683885904.
E-mail address: cplucumt@126.com (C.-P. Lu).

1365-1609/$ - see front matter
doi:10.1016/j.ijrmms.2010.06.009

predicted the blast-induced ground vibration and frequency by incorporating rock properties, blast design and explosive parameters using the ANN technique. Ju et al. [11] presented the experimental and theoretical investigations of property of stress wave propagation in jointed rocks by means of SHPB technique and fractal geometry method. Ak and Konuk [12] examined the impacts of the discontinuity frequency parameter derived through geological measurements on the blasting benches or nearby in a quarry mine on the propagation of blast-induced ground vibrations. Wang et al. [13] studied the effects of soft porous layer barriers on the reduction of buried blast-induced ground shock based on the prototype dimensions of a centrifuge test. Zhu et al. [14] discussed the influences of the factors of boundary condition, coupling medium, borehole diameter, decoupling and joint on rock dynamic fracture. Chafi et al. [15] accurately studied the blast wave propagation in the medium and the response of the structure to blast loading. Kuzu et al. [16] put forward a method of modified scaled distances (SDs) based on empirical equations considering factors such as blasting and geological parameters of rock mass for bench blasting in quarries. Chen and Zhao [17] found that the joints in the rock masses produced fast attenuation of the blast wave propagation with UDEC Modelling. Tian et al. [18] discussed the frequency spectrum characteristics of blast-induced shock wave from foundation pit excavation, and revealed that the frequency change rule in relation to blasting distance, charge volume, blasting method and elevation. Zhang et al. [19] discovered that the blast-induced micro-fissure can restrain high-frequency vibration wave, and the frequency mainly distributed in low-frequency band (20–95 Hz). Gao et al. [20] studied energy attenuation in relation to the propagation distance by microseismic (MS) tests in different media on the surface. Ye et al. [21] conducted a field monitoring experiment on the wave propagation from an explosive source in a deep coal mine. The results showed that MS attenuation is exponentially related to the propagation distance.

As a consequence of the above, blast-induced shock wave propagation and attenuation laws in different mechanical characteristics of coal and rock media have been researched by extensive experiments in detail, especially, the correlation between the PPV and the main frequency spectrum of MS signals has been discussed fruitfully, the foundation on evaluating the stability and safety of surface buildings induced by blasting has been established. However, for three-component signals of blast-induced shock wave, the propagation and attenuation laws in coal and rock media and the frequency spectrum evolution laws still lack field experimental studies.

By a total of about 180 three-component recordings, the three-component signals propagation and attenuation, and frequency spectrum evolution rules of blast-induced shock waves were studied under the guidance of KZ-1 MS monitoring system developed by China's State Seismological Bureau, in the headentry drilling process of 7206 working face in Sanhejian Coal Mine (SCM) located in Xuzhou city, and the relationship between the main frequency spectrum and the stress concentration of coal and rock materials were revealed as well in this paper.

2. Test apparatus, conditions and blasting parameters

2.1. Introduction of MS monitoring system

The KZ-1 MS monitoring system was developed by the institute of geophysics, China's State Seimological Bureau. There are twelve seismometers installed in the whole mining area, ten of them were arranged underground, the other two seismometers named Meiqizhan and Luxinzhuang were installed in two ground-based deep boreholes, with hole depths of 228 and 229 m, respectively. The frequency band of the seismometer is 5–100 Hz. MS signals transmit by the optical cable, while each seismometer collects on three-directional components that include four signal channels. The sampling rate is 1000 sps, and the dynamic range is greater than 100 dB. The vertical component includes two signal channels, while the total dynamic range is greater than 140 dB. The MS events, with magnitude above -2.0 taken place in monitoring areas, can be detected by lower threshold; the recording type uses a trigger mode. Based on the theory of D-optimal design and localization, the preliminary location program of MS monitoring network was formed, which was evaluated using numerical emulation experiment on the basis of statistics, and was also tested eventually by the measured and artificial experimental data, then a suitable network layout of SCM MS monitoring system was obtained. Fig. 1 shows the MS network layout of SCM. The surface average elevation is +36 m. 8# seismometer is named Meiqizhan, and 12# seismometer is named Luxinzhuang.

2.2. Test condition

SCM is one of the most serious rockburst coal mines in China. The first rockburst hazard happened in 7110 working face headentry in 1991. The destructive rockburst has taken place more than 25 times till now. Especially, a rockburst hazard happened in 7204-3 working face on December 6, 1998, which destroyed 500 m long roadway, which resulted in closing the working face. Another case, at 15:25 on April 17, 2000, a rockburst of magnitude 3.0 happened in 7204 working face. 180 m long coal wall was damaged and four workers were killed in the disaster. Now, the rockburst has been one of the major coal and rock dynamic disasters in SCM. As the mining depth increases, the rockburst danger becomes more severe.

The field experimental study was conducted in the headentry of 7206 working face, while the average elevation of 7206 working face headentry is -840 m, 6 three-component seismometers were installed around 7206 working face headentry, viz. 1#, 3#, 4#, 8#, 10# and 12#. This experimental study mainly analyzed MS data collected by the 1#, 3# and 4# seismometer stations. In the initial driving of headentry, the shock waves of explosive sources were collected by the nearest 1# seismometer. With continuous driving, the propagation and attenuation laws of three-component signals of blast-induced shock wave were measured.

2.3. Blasting parameters

A 5 m width coal pillar was left between the headentry of 7206 working face and the nearby 7204 working face's tailentry. Both the sides, except for the gob side, which 7204 working face had mined out, were real coal materials. Blasting is the normal driving shot. Generally, 5–6 holes were drilled ahead of the headentry of 7206 working face, and the total charge weight was about 12–15 kg, which was detonated simultaneously. Fig. 2 is the plane sketch of the headentry drilling of 7206 working face.

3. Results and discussions

3.1. Differences in shock wave transverse and bed-parallel propagations

The blast-induced shock wave propagation process is extremely complex. There are many factors that influenced the wave

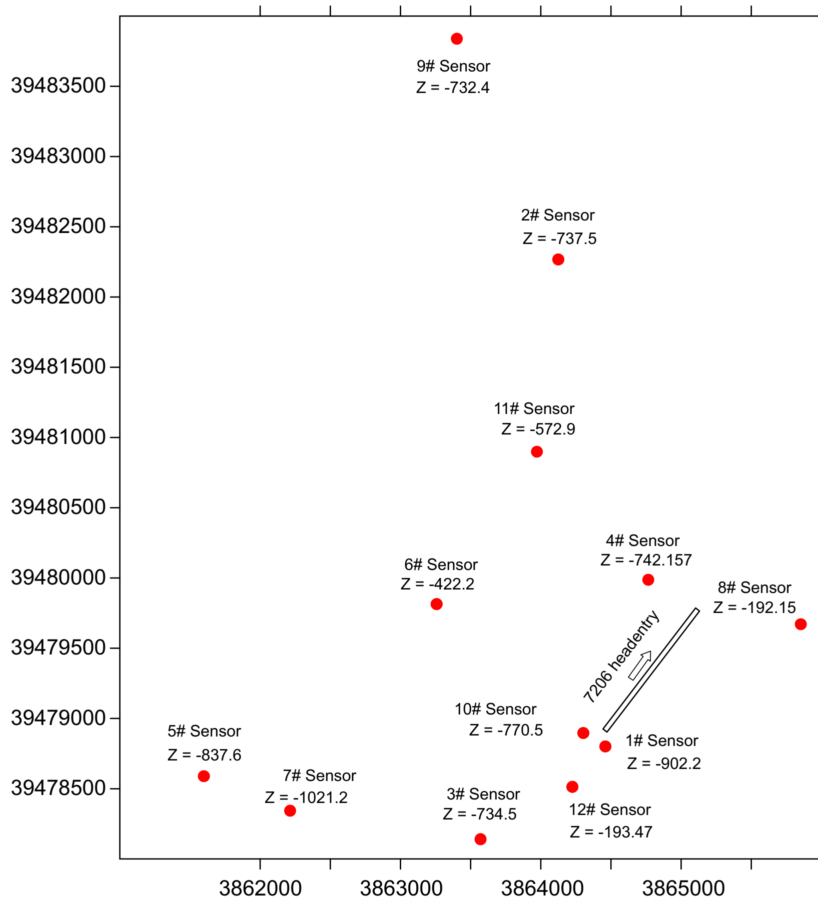

Fig. 1. Distribution of MS stations in SCM.

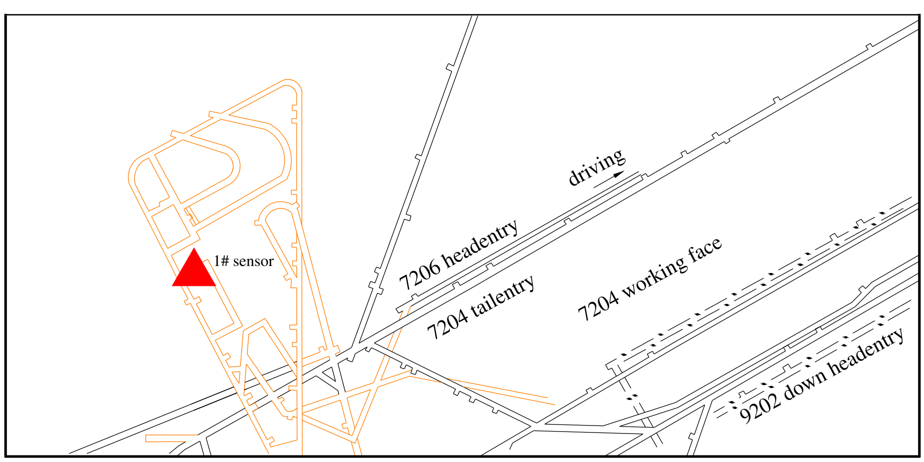

Fig. 2. Plane sketch of the headentry driving of 7206 working face.

energy loss, such as propagation distance, ray path, medium mechanic property, rock joints, etc. According to the small-scale coal and rock materials, based on the measured data by tests, combined the correlation between the seismometers and explosive source, the energy attenuation differences in three-component signals between the transverse and bed-parallel propagations were presented. So-called transverse propagation, which is the single-component wave goes through a number of interfaces among the coal and rock layers from explosive source to seismometers, when each wave passes an interface, accompanied by reflection, refraction and diffraction processes, the energy of wave will rapidly attenuate. That single-component wave does not go through the interfaces among the coal and rock layers from explosive source to seismometers is so-called bed-parallel propagation, and the wave spreads in a single coal or rock layer. Compared to transverse propagation, the energy loss is less.

3.2. *Three-component characteristics of explosive source signals*

To study the energy and frequency attenuation differences between the transverse and bed-parallel propagation of the three-component signals of blast-induced shock wave, the amplitude-time curves of three-component signals must be collected by tests, then, the three-component characteristics of the explosive source signals can be revealed. So, we decided to collect the explosive source shock wave with the nearest 1# seismometer in the initial driving of the headentry. Fig. 3 shows the energy and frequency distribution curves of three-component signals of blast-induced shock wave collected by 1# seismometer.

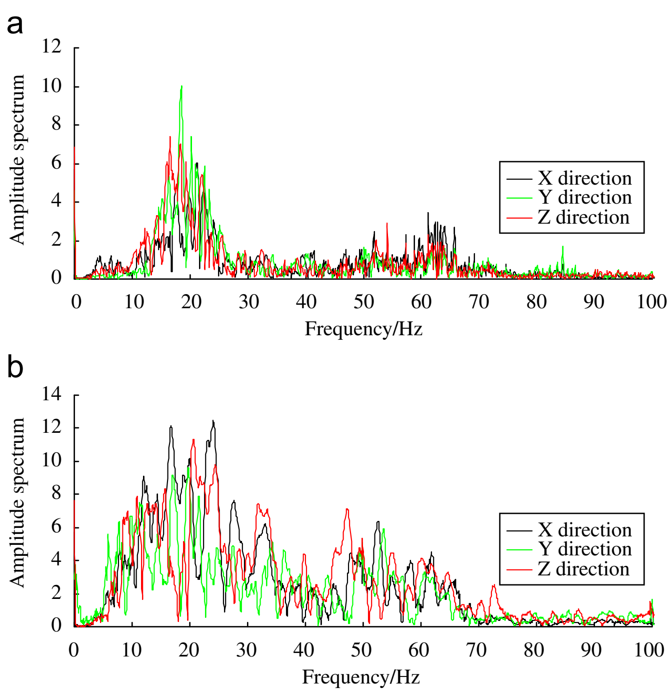

Fig. 3. Energy and frequency distribution curves of the three components of blast-induced shock wave signals (1# seismometer). (a) Blasting signal at 10:42 on October 3, 2008. (b) Blasting signal at 10:55 on October 5, 2008.

As seen from Fig.3, we can find that the horizontal energy and frequency distributions of shock wave of the nearby explosive source are approximately same as that of the vertical ones. The main frequency of the signals is between 0 and 70 Hz. The low-frequency (0–40 Hz) signals are mainly produced by explosion, while the high-frequency components (40–70 Hz) are mainly produced by a large number of micro-cracks generation, expansion and convergence induced by explosion.

3.3. *Three-component signals propagation and attenuation characteristics of shock wave*

In order to reveal the propagation and attenuation laws of three-component signals of the blast-induced shock wave in coal and rock medium, the attenuation laws of transverse and bed-parallel propagation in the far zone were measured, based on the propagation distance change of explosive source to 1#, 3# and 4# seismometers in the process of 7206 headentry driving.

Test 1: we drilled 5 blast holes in the headentry of 7206 working face on October 6, 2008, the total charge weight was 15 kg, and the detonation was at 10:31 AM. Fig. 4 is the location relation sketch between the source and 1#, 3# and 4# seismometers. Fig. 5 is shock wave energy and frequency distribution curves of three-component signals. In Fig. 4, the horizontal distance of source to 3# seismometer is about 3.5 times than that of it to 1# seismometer, and is approximately equal to the distance between source and 4# seismometer.

From the figures above, with transverse and bed-parallel propagation of three-component signals of shock wave, the high-frequency components rapidly attenuated, and spectrum moved to low-frequency band. Because of the different attenuation indexes of transverse and bed-parallel propagations, when the horizontal propagation distance increase was about 3.5 times, the energy attenuation was nearly 5 times (Fig. 5a,b). But when the vertical propagation distance increase was about 3 times, the

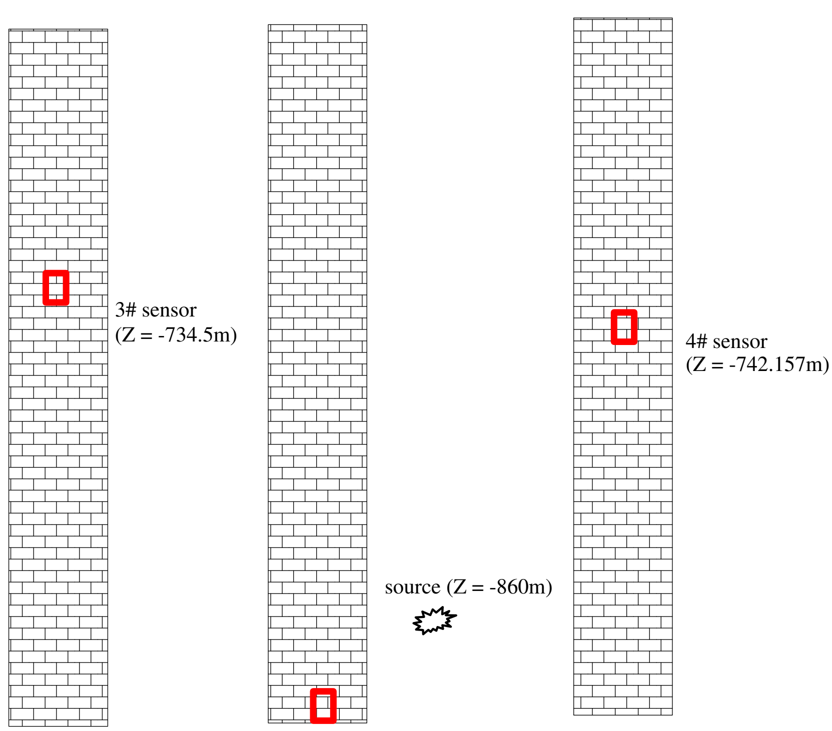

Fig. 4. Location relation sketch between source and 1#, 3#, 4# seismometers (October 6).

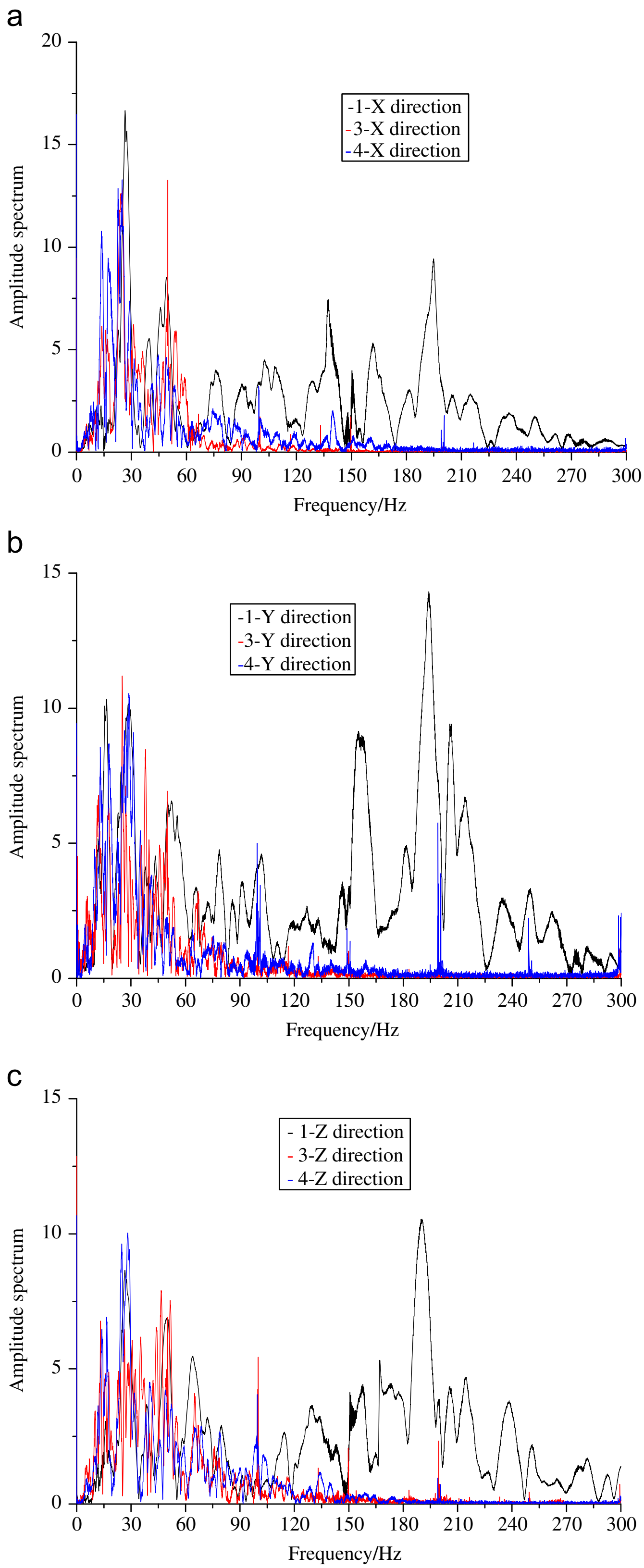

Fig. 5. Energy and frequency distribution curves of three-component signals of shock wave (October 6). "1-*X* direction" in (a) reduced to 1/5 of origin value. "1-*Y* direction" in (b) reduced to 1/5 of origin value. "1-*Z* direction" and "4-*Z* direction" in (c) reduced to 1/8 and 1/2 of origin value, respectively. (a) Horizontal *X* direction, (b) horizontal *Y* direction, (c) vertical *Z* direction.

energy attenuation was nearly 8 times (Fig. 5c). According to the vertical-directional energy of 3# and 4# seismometers, both of the horizontal propagation distances were equal, and there was only a 7.6 m gap between both the vertical propagation distances, but the residual *Z*-directional energy of 4# seismometer was about 2 times as much as it of 3# seismometer.

Test 2: we drilled 6 blast holes in the headentry of 7206 working face on October 16, 2008, the total charge weight was 15 kg, and the detonation was at 10:54 AM. After explosion, about 4–5 t coal in the center of head-on was ejected, the farthest ejection distance was about 10 m. Fig. 6 shows the location relation sketch between source and 1#, 3# and 4# seismometers, Fig. 7 shows the shock wave energy and frequency distribution curves of three-component signals. In Fig. 6, the horizontal distance of source to 3# seismometer is about 1.67 times than that of it to 4# seismometer.

From the figures above, according to the horizontal-directional energy of 3# and 4# seismometers, when the horizontal propagation distance increase was about 1.67 times, the energy attenuation was nearly 2 times (Fig. 7a,b). But based on vertical-directional energy of 3# and 4# seismometers, the horizontal propagation distance of 3# seismometers was about 1.67 times as much as it of 4# seismometer, and there was only a 7.6 m gap between both the vertical propagation distances, but the residual *Z*-directional energy of 4# seismometer was about 6 times likely as much as it is of 3# seismometer. Compared to test 1, the horizontal propagation distance has a noticeable effect on the vertical-directional energy attenuation.

As a consequence of the above, when blast-induced shock wave propagates in coal and rock media, with increase in propagation distance, the high-frequency components rapidly attenuate, and the main frequency distribution is 0–60 Hz. According to the attenuation index, the vertical attenuation index of transverse propagation is larger than bed-parallel horizontal attenuation index. Especially, the horizontal propagation distance has a noticeable effect on the vertical-directional energy attenuation.

Fig. 8 shows the relation between the main frequency and the corresponding attenuation coefficients, as an example of relieve-shot on October 6.

From the above figure it was found that the higher the frequency of blast-induced shock wave signal was, the bigger the attenuation coefficient of amplitude spectrum was. For the horizontal-directional shock wave signals, when the main frequency was higher than 60 Hz, the attenuation coefficient of spectrum energy began to increase dramatically. But for the vertical-directional shock wave signals, the spectrum energy attenuation threshold value was about 120 Hz.

3.4. Relation between frequency spectrum and the stress concentration of coal and rock

Tests process: (1) we drilled 6 blast holes in the headentry of 7206 working face on October 19, 2008, the total charge weight was 15 kg, and the detonation was at 10:35 AM. (2) a rock burst happened in the headentry at 7:05 on October 29, 2008, which destroyed the coal wall of head-on, and six workers were wounded by the coal and ejection of the rock bricks. To control the rockburst strength, 5 blast holes were drilled in the headentry of 7206 working face, the total charge weight was 12 kg, and the detonation was at 10:18 AM. Fig. 9 shows the frequency spectrum distribution curves of three-component signals of 1# seismometer.

From the figures above, the main frequency distribution is about 0 – 50 Hz collected on October 19. The central frequency is

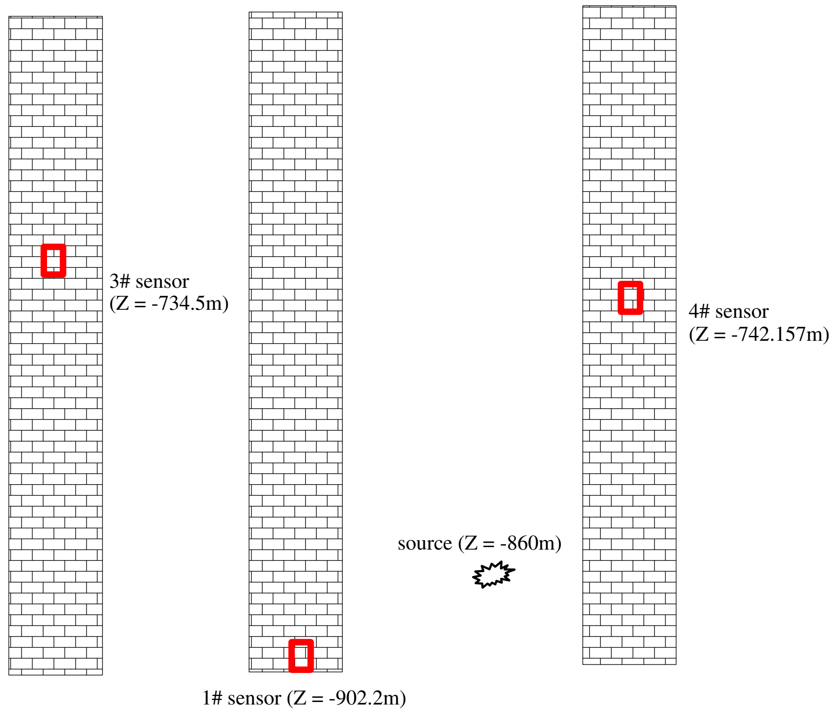

Fig. 6. . Location relation sketch between the source and 1#, 3#, 4# seismometers (October 16).

lower, compared to the frequency spectrum distribution (0−70 Hz) of explosive source signal that a large number of micro-cracks and macro-fracture converged cannot be produced in the coal and rock materials after explosion can be known. So, the stress of coal and rock materials does not reduce, and the elastic energy accumulated cannot be effectively released. The main frequency distribution is about 0−200 Hz on October 29, the high-frequency components (100−200 Hz) significantly increase. Based on the propagation and attenuation laws of blast-induced shock wave, according to 1# seismometer, even the total charge weight difference is small, the propagation distance on October 29 is greater than that on October 19, so the main frequency of signals on October 29 should be lower than that on October 19, but on the contrary in fact that blasting produces a large number of micro-cracks and macro-fracture in the coal and rock materials, which can be illustrated on Oct 29, while the micro-cracks produce the high-frequency signals, and the elastic energy accumulated can be effectively released, then the stress concentration level will reduce.

To verify the relation between frequency spectrum distribution and the mechanic characteristics of the coal and rock materials after explosion, drilling bits volume of different locations in head-on was measured before and after every explosion. Figs. 10 and 11 are the curves of drilling bits volume before and after two relieve-shots, respectively.

On October 20, the measured drilling bits volume not only has not been reduced, but also shows a gradual upward trend after explosion, which illustrates that blasting does not reduce the stress concentration of the coal and rock materials; thus the accumulated elastic energy cannot be released, and the relief result is not obvious.

On October 30, the measured drilling bits volume rapidly reduces after explosion, especially when drilling depth is 4 m, 3.6 m upward in head-on, drilling bits volume reduces from 21.9 to 7.6 kg/m, which illustrates that blasting releases the elastic energy and reduces the stress concentration, and the relief result is very obvious.

As a consequence of the above, when 100–200 Hz high-frequency signals of shock wave significantly increase, which shows that blasting induces to form a number of micro-cracks, and the explosive energy and elastic energy released together promotes convergence and connectivity among micro-cracks to form macro-fracture. So, the stress peak position of coal and rock materials will move to deep, and the stress concentration level will reduce.

In conclusion, it was also found that the more loose and broken coal and rock material was, the more obvious shock wave energy attenuation was. In the rockburst dangerous areas, the deep-hole relieve-shot was adopted as a main method to reduce the strength and integrity of coal and rock material, so its absorption capacity for the residual energy of rockburst shock wave was raised, the stress peak position will move to deep, thereby the rockburst danger can be weakened and reduced.

4. Conclusions

By the normal production explosion in the period of headentry drilling of 7206 working face in SCM, the propagation and attenuation laws of blast-induced shock wave were studied by experiments in field, especially the relationship between the frequency spectrum distribution and the stress concentration of coal and rock materials after explosion was revealed. The main conclusions were as follows:

(1) The horizontal and vertical energies and frequency distribution of nearby explosion source shock wave are approximately equal. The main frequency distribution is about 0–70 Hz, and 0–40 Hz low-frequency signals are mainly produced by blast-induced shock wave, while the high-frequency components (40–70 Hz) are mainly produced by a large number of micro-cracks generation, expansion and convergence.
(2) When the blast-induced shock wave propagates in coal and rock media, the high-frequency components rapidly attenuate

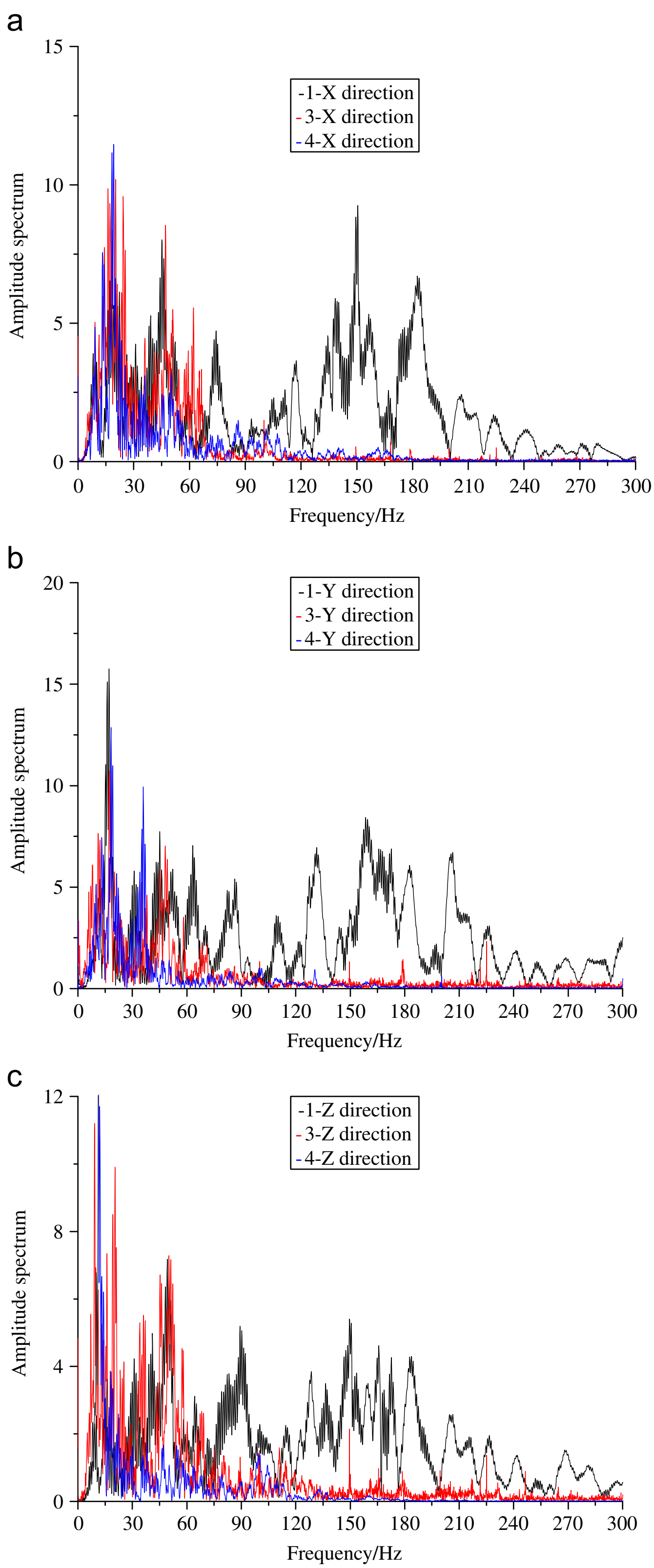

Fig. 7. Energy and frequency distribution curves of three-component signals of shock wave (October 16). "1-*X* direction" and "4-*X* direction" in (a) reduced to 1/5 and 1/2 of origin value, respectively. "1-*Y* direction" and "4-*Y* direction" in (b) reduced to 1/5 and 1/2 of origin value, respectively. "1-*Z* direction" and "4-*Z* direction" in (c) reduced to 1/8 and 1/6 of origin value, respectively. (a) Horizontal *X* direction, (b) horizontal *Y* direction, (c) vertical *Z* direction.

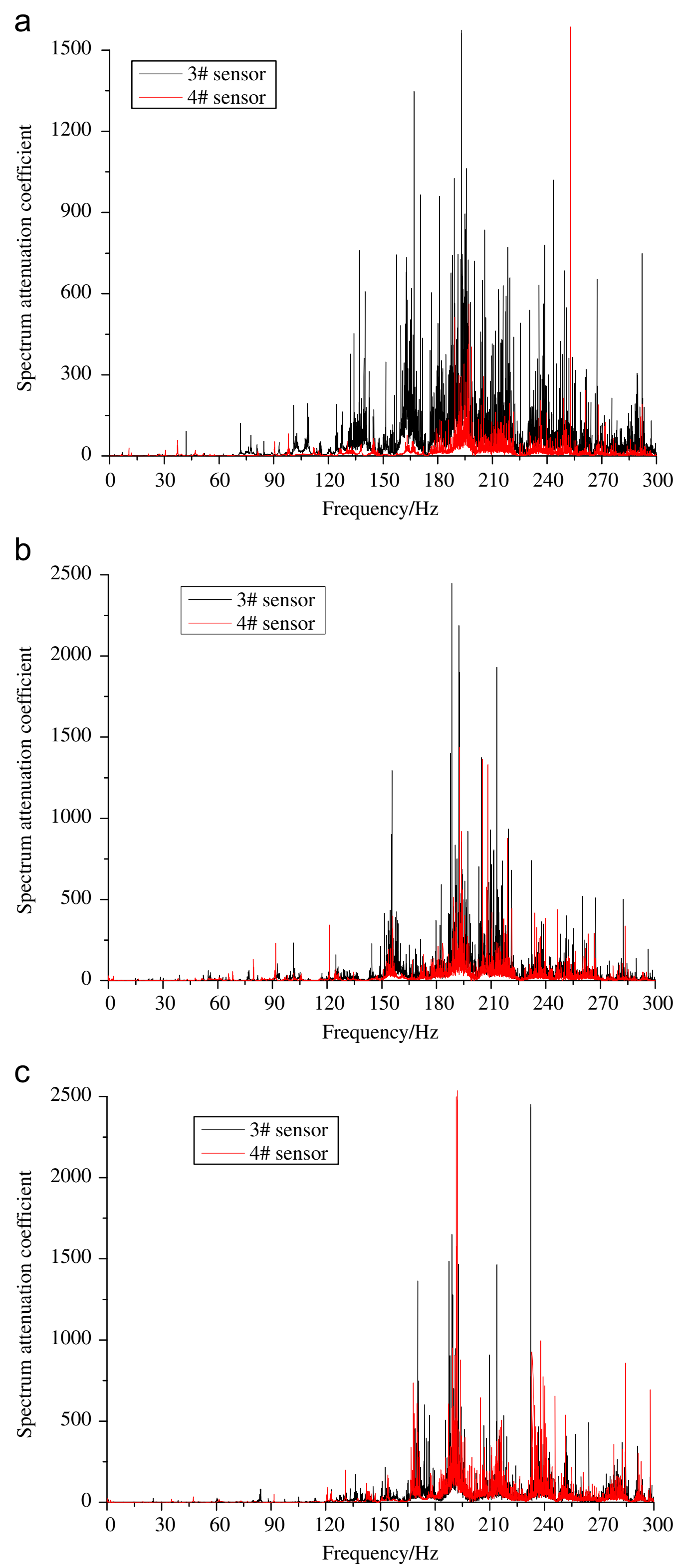

Fig. 8. Relation between main frequency and the corresponding attenuation coefficients (October 6). (a) Horizontal *X* direction, (b) horizontal *Y* direction, (c) vertical *Z* direction.

with increase in propagation distance, and the main frequency distribution is about 0–60 Hz. According to the attenuation coefficient, the vertical attenuation coefficient of transverse propagation is bigger than bed-parallel horizontal attenuation coefficient. Especially the horizontal propagation distance has a noticeable effect on vertical energy attenuation.

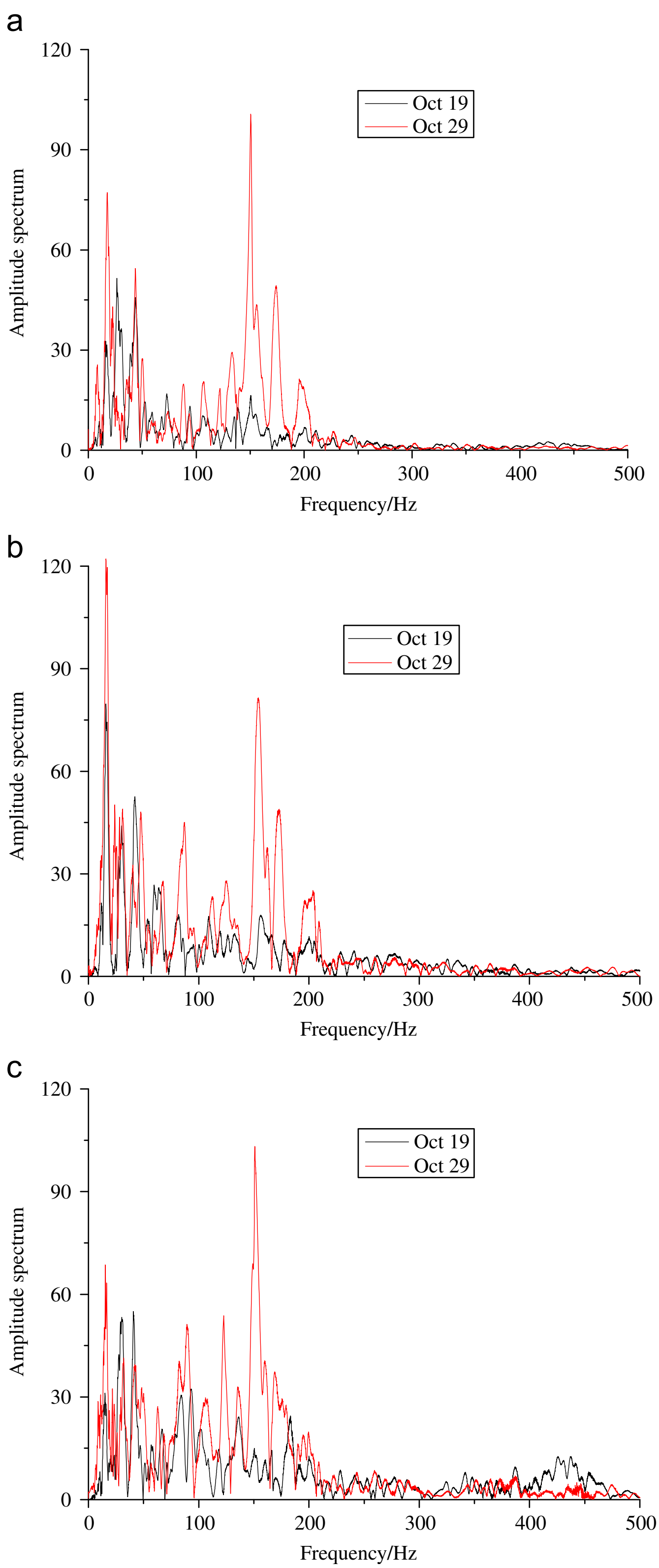

Fig. 9. Frequency spectrum distribution curves of three-component signals. (a) Horizontal *X* direction, (b) horizontal *Y* direction, (c) vertical *Z* direction.

(3) The higher the frequency of shock wave signal is, the bigger the energy attenuation coefficient is. For horizontal shock wave signals, when the main frequency is higher than 60 Hz, the attenuation coefficient begins to increase dramatically. But for vertical shock wave signals, the energy attenuation threshold value is about 120 Hz.

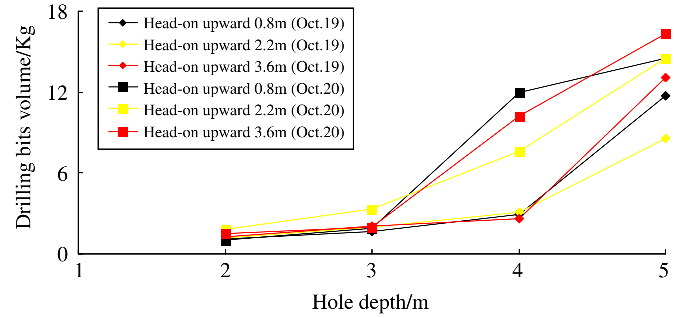

Fig. 10. Change curve of drilling bits volume before and after relieve-shot (October 19).

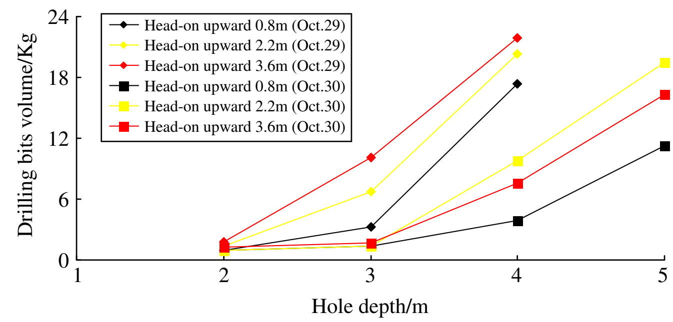

Fig. 11. Change curve of drilling bits volume before and after relieve-shot (October 29).

(4) When 100–200 Hz high-frequency signals of shock wave significantly increase, which means that blasting produces a number of micro-cracks, and the explosive energy and elastic energy released together promotes convergence and connectivity among micro-cracks to form macro-fracture. So, the stress peak position of coal and rock materials will move to deep, and the stress concentration level will reduce.

Acknowledgements

First, we are grateful to the editor and two unknown referees for suggestions which improved the quality of this note. Second, we wish to acknowledge the collaborative funding support from the National Key Project of Scientific and Technical Supporting Programs (2006BAK04B02, 2006BAK03B06), 973 National Basic Research Program (2010CB226805). In particular we wish to thank Gong Siyuan, Cao Anye, He Hu, Chen Ligao and He Gang for their contributions to this research project.

References

[1] Ak H, Iphar M, Yavuz M, Konuk A. Evaluation of ground vibration effect of blasting operations in a magnesite mine. Soil Dyn Earthquake Eng 2009;29:669–76.
[2] Tantawy MM. Artificial neural network for prediction and control of blast-induced shocks in Assiut (Egypt) limestone quarry. Int J Rock Mech Min Sci 2009;46:426–31.
[3] Holub K, Petroš V. Some parameters of rockbursts derived from underground seismological measurements. Tectonophysics 2008;456:67–73.
[4] Wu YK, Hao H, Zhou YX. Propagation characteristics of blast-induced shock waves in a jointed rock mass. Soil Dyn Earthquake Eng 1998;17:407–12.
[5] Kuzu C. The importance of site-specific characters in prediction models for blast-induced ground vibrations. Soil Dyn Earthquake Eng 2008;28:405–14.
[6] Khandelwal M, Singh TN. Prediction of blast induced ground vibrations and frequency in opencast mine: a neural network approach. J Sound Vib. 2006;289:711–25.
[7] Wang ZL, Li YC, Wang JG. A method for evaluating dynamic tensile damage of rock. Eng Fract Mech 2008;75:2812–25.

[8] Hao H, Wu YK, Ma GW, Zhou YX. Characteristics of surface ground motions induced by blasts in jointed rock mass. Soil Dyn Earthquake Eng 2001;21: 85–98.
[9] Uysal O, Erarslana K, Cebi MA, Akcakoca H. Effect of barrier holes on blast induced vibration. Int J Rock Mech Min Sci 2008;45:712–9.
[10] Khandelwal M, Singh TN. Prediction of blast-induced ground vibration using artificial neural network. Int J Rock Mech Min Sci 2009;46:1214–22.
[11] Ju Y, Sudak L, Xie HP. Study on stress wave propagation in fractured rocks with fractal joint surfaces. Int J Solids Struct 2007;44:4256–71.
[12] Ak H, Konuk A. The effect of discontinuity frequency on ground vibrations produced from bench blasting: a case study. Soil Dyn Earthquake Eng 2008;28:686–94.
[13] Wang JG, Sun W, Anand S. Numerical investigation on active isolation of ground shock by soft porous layers. J Sound Vib. 2009;321: 492–509.
[14] Zhu ZM, Mohanty B, Xie HP. Numerical investigation of blasting-induced crack initiation and propagation in rocks. Int J Rock Mech Min Sci 2007;44:412–24.
[15] Chafi MS, Karami G, Ziejewski M. Numerical analysis of blast-induced wave propagation using FSI and ALE multi-material formulations. Int J Impact Eng 2009;36:1269–75.
[16] Kuzu C, Fisne A, Ercelebi SG. Operational and geological parameters in the assessing blast induced airblast-overpressure in quarries. Appl Acoust 2009;70:404–11.
[17] Chen SG, Zhao JA. Study of UDEC modelling for blast wave propagation in jointed rock masses. Int J Rock Mech Min Sci 1998;35:93–9.
[18] Tian YS, Li ZJ, Wang XG, et al. Spectra characteristics of blast-induced shock wave from foundation pit excavation. Blasting 2005;22(29-31):50.
[19] Zhang QS, Li LP, Li SC, et al. Experimental study of blasting dynamic vibration of closely adjacent tunnels. Rock Soil Mech 2008;29:2655–60.
[20] Gao MS, Dou LM, Zhang N, et al. Experimental study on earthquake tremor for transmitting law of rockburst in geomaterials. Chin J Rock Mech Eng 2007;26:1365–71.
[21] Ye GX, Jiang FX, Guo YH, et al. Experimental research on seismic wave attenuation by field microseism monitoring in a deep coal mine. Chin J Rock Mech Eng 2008;27:1053–8.